Contribution to the Understanding of Austenite Stability in a 12Cr-9Ni-4Mo Maraging Steel

David San Martin[1a], Niels van Dijk[2b], Yuriy Yagodzinskyy[3c], Ekkes Brück[4d], Sybrand van der Zwaag[1e]

[1]*Fundamentals of Advanced Materials Group, Faculty of Aerospace Engineering, TU Delft, Kluyverweg 1, 2629 HS Delft, The Netherlands*
[2]*Fundamental Aspects of Materials and Energy, Faculty of Applied Sciences, TU Delft, Mekelweg 15, 2629 JB Delft, The Netherlands*
[3]*Helsinki University of Technology, Laboratory of Engineering Materials, FIN-02150 Espoo, Finland*
[4]*Van der Waals-Zeeman Institute, University of Amsterdam, Valcknierstraat 65, 1018 XE Amsterdam, The Netherlands*

[a] D.M.SanMartin@LR.TUDelft.NL, [b] N.H.vanDijk@IRI.TUDELFT.NL, [c] Yuriy.Yagodzinskyy@hut.fi, [d]bruck@science.uva.nl, [e] S.vanderZwaag@LR.TUDelft.NL.

(NOTE Since 2008, David San Martín works at the National Centre for Metallurgical researcher (CENIM-CSIC) in Madrid, Spain. E-mail: dsm@cenim.csic.es).

Keywords: Martensitic transformation, Austenite, Internal Friction, Magnetic Measurements, Neutron Depolarization.

Abstract. Maraging steels show an excellent combination of high strength and ductility, which makes them very attractive in a large variety of potential applications. The present work is concerned with the main factors influencing the stability of metastable austenite in such a steel. At subzero temperatures a large variation in the isothermal transformation behaviour of austenite to martensite has been observed. Factors such as the austenite grain size and the interstitial content in solid solution are known to influence austenite stability and, therefore, the martensitic transformation. In this steel, the addition of titanium results in carbonitride precipitation. These precipitates play an indirect but important role in the stability of austenite by means of removing interstitials from the solid solution and by inhibiting an austenite grain growth. The combination of techniques such as X-ray diffraction, magnetisation measurements, three-dimensional neutron depolarisation, and internal friction measurements enables a complete characterisation of the transformation. A step towards understanding the factors responsible for the variation in the behaviour observed is the main contribution of this work.

Introduction

It is well known that the austenite to martensite transformation in Fe-based alloys can proceed athermally, as a function of temperature; isothermally, as a function of temperature and time; or by plastic deformation (strained-induced martensite) [1, 2, 3]. The isothermal reaction generally occurs below the martensitic start temperature, M_S, but there are examples of martensite forming isothermally also above M_S [1]. The formation of isothermal martensite is characterized by C-curve kinetics, with the nose of the curve usually at different subzero temperatures depending on the composition of the alloy [1]. By contrast, athermal martensite takes place during cooling only when the M_S temperature is reached. Further transformation on cooling takes place until the reaction ceases at the M_F temperature. These critical temperatures can vary over a wide temperature range depending on composition [4]. While athermal martensite forms usually by growth of already existing plates, isothermal martensite develops by continual nucleation of new plates [5, 6]. In some austenitic stainless steels both athermal and isothermal martensite may occur. Fe-Ni-Mn and Fe-Ni-Cr alloys are known as typical examples of such materials [1]. Steels with an austenitic

microstructure at room temperature, can also transform to martensite after cold-working [3]. Strain-induced martensite predominantly appears inside austenite grains at the intersection of shear bands. This mechanism was explained by Olson and Cohen [7].
Previous studies concerning the martensitic transformation in austenitic stainless steels used X-ray diffraction (*XRD*) to determine the martensite volume fraction [8, 9]. However, this technique may have some limitations due to the influence of textures on the interpretation of the measurements. Magnetic methods like magnetization and three-dimensional neutron depolarization (*3DND*) measurements [9-12] are good alternative tools to characterize phase transformations in steels taking advantage of the fact that austenite is paramagnetic phase, while martensite exhibits ferromagnetic behaviour. Magnetization measurements enable the determination of the magnetic phase fraction when the saturation magnetization of martensite is known. The advantage of magnetisation measurements in comparison with X-ray diffraction measurements is that the determination of the phase fraction is relatively insensitive to texture when the applied magnetic fields are sufficiently high. The *3DND* technique is based on the precession of the neutron beam polarization during transmission through a ferromagnetic phase. This method can simultaneously probe the magnetic phase fraction and the average magnetic domain size. In order to obtain the average martensite grain size the applied field should be sufficiently large to have a single magnetic domain inside the martensite grain [13]. The magnetic phase fraction however can only be determined in relatively low applied magnetic fields due to a loss of the neutron beam polarisation for large stray fields.

Two main factors influence the martensitic transformation kinetics for a given composition; the grain size and the interstitial impurities [5, 14]. The austenite grain size can be controlled by adjusting the austenitization conditions at high temperature before cooling to room temperature. A prediction of the amount of free interstitials is more complex. Many investigations have been made on the effects of alloying elements on the solubility and precipitation of carbon and nitrogen in steels [15]. The application of cyclic micro-stresses to study the damping or internal friction behaviour of steels is a powerful technique to examine the behaviour and state of interstitials in steels. Snoek was the first to show that the damping behaviour observed in ferritic steels was due to the presence of free interstitial solutes (carbon and nitrogen) in solid solution in ferrite [16]. Internal friction peaks in steels have been observed at different temperature locations depending on composition, deformation state and phases present in the matrix [17, 18]. These peaks are the result of a relaxation phenomenon associated with the redistribution of interstitial atoms in the matrix under the application of oscillatory micro-stresses. Golovin et al. have also shown that IF measurements can be used to study the isothermal martensitic transformation [19].

Although the austenite-martensite transformation is reasonably well understood and documented, in the industrial practice an unexpected variation in transformation behaviour has been reported. The combination of several different techniques such as X-ray diffraction, magnetisation measurements, three-dimensional neutron depolarisation, and internal friction measurements can potentially enable a complete characterisation of the transformation. This could lead towards a better understanding of the factors responsible for the variation in the behaviour observed.

Materials and Experimental Procedure

The composition of the steel used in this work was determined by X-ray fluorescence and is given in Table 1. The as-received material was delivered as strips of 48 mm length × 31 mm width × 0.5 mm thickness. The M_S temperature of this steel is as low as 77 K [20] and the nose of the C-curve is around 233 K [14]. The microstructure of the as-received material is mainly composed of austenite, but two other phases are also present: (1) a small amount of transformed martensite and (2) the χ phase ($Fe_{36}Cr_{12}Mo_{10}$) precipitated in the matrix (Fig. 1a). Fig. 1b shows some martensite present in the initial microstructure. The mean austenite grain size (*AGS*) was revealed using a variation of

dilute aqua regia (3 parts HCl, 2 parts water, 1 part HNO_3) and long periods of etching. The AGS was measured using an image analyzer. The mean diameter determined was 5 µm.

Table 1. Chemical composition of the studied steel [wt.%] with balance Fe.

Cr	Ni	Mo	Ti	Al	Si	Cu	Mn	Co	V	S	P	C	N
11.4	8.7	3.4	1.1	0.7	0.3	2.5	0.3	0.08	0.06	0.04	0.03	0.008	0.006

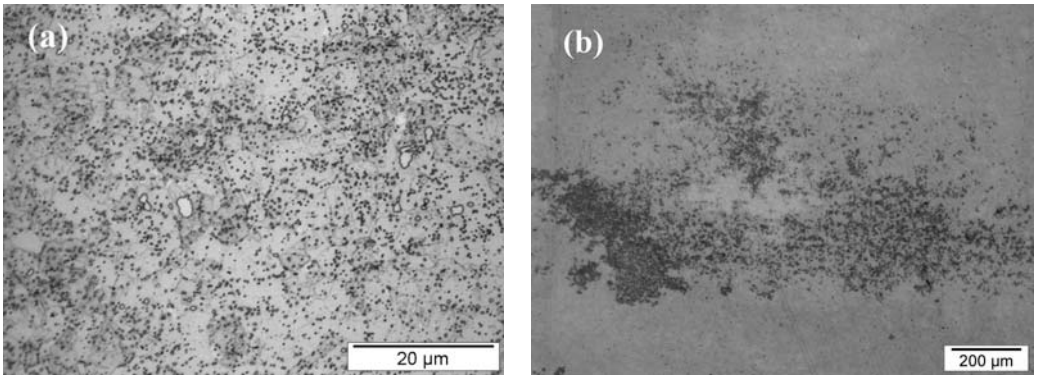

Fig. 1 Optical micrographs. (a) White and black dots are χ phase ($Fe_{36}Cr_{12}Mo_{10}$) precipitated in the austenitic matrix. (b) Isothermally transformed martensite (darker phase) in austenite.

Although the composition and grain size was the same for all samples, transformation behaviour was found to be different for samples taken from different coils. Samples called B have poorer transformation behaviour than samples A. In order to study the martensitic transformation, square samples of 15 mm in length and smaller rectangular samples of 2 mm × 3 mm, taken from both locations in the strip, were treated isothermally at 233 K for different periods of time (4, 8, 12, 16, and 48 h). The obtained microstructure was then analyzed using *XRD* and *3DND* measurements (square samples) and magnetisation measurements (rectangular samples). The *XRD* measurements were performed on a Bruker-AXS D8 advance diffractometer equipped with a Bruker Vantec position sensitive detector and Co-Kα radiation. The magnetization measurements were performed at room temperature with a MagLab system (Oxford Instruments), which consist of a 9 Tesla superconducting magnet equipped with a Variable Temperature Insert (*VTI*) for measurements at temperatures between 2 and 360 K. The *3DND* experiments were performed on the instrument PANDA at the Reactor Institute Delft. Temperature dependent internal friction Q^{-1} was measured by and inverted torsion pendulum in the temperature range of 95-500K in the Laboratory of Engineering Materials at the Helsinki University of Technology. Specimens were heated at a constant rate of 2 K/min. The frequency of the pendulum was varied between 1.7 and 2.0 Hz. Sample dimensions used for the internal friction measurement were 45 mm length × 2.5 mm width × 0.5 mm thickness.

Results and Discussion

Figure 2 presents the evolution of the *XRD* diffraction spectra for as-received and two holding times (12 and 48 h) at 233 K for samples A and B. From the comparison of the peak heights it is clear that the martensitic transformation behaviour is different for the two samples. Due to the small initial *AGS* (5 µm) the transformation kinetics is very slow and only a small fraction of martensite has been transformed after 48 hours. The quantitative estimation of the phase fractions is based on the principle that the total integrated intensity of all diffraction peaks for each phase in a mixture is proportional to the volume fraction of that phase [21, 22]. In Table 2, the volume fraction of martensite present in the microstructure measured with XRD is given for samples A and B.

In order to obtain a more reliable quantification of the martensitic transformation, bulk analysis techniques can be used. In order to avoid the effect of a possible transformation at the surface during machining and suppress the influence of texture high-field magnetization measurements have been performed. This method is based on the measurement of the saturation magnetization of the sample, M_S, which can be obtained from the high field limit of the magnetization curves as a function of the applied magnetic field. For the steel composition listed in Table 1 the saturation magnetization of pure martensite, M_S^m, corresponds to about $\mu_0 M_S^m \approx 1.8$ T [23]. The volume fraction of martensite can be calculated by the following simple equation, $f_m = M_S^t / M_S^m$, where M_S^t is the saturation value of the sample at a given time.

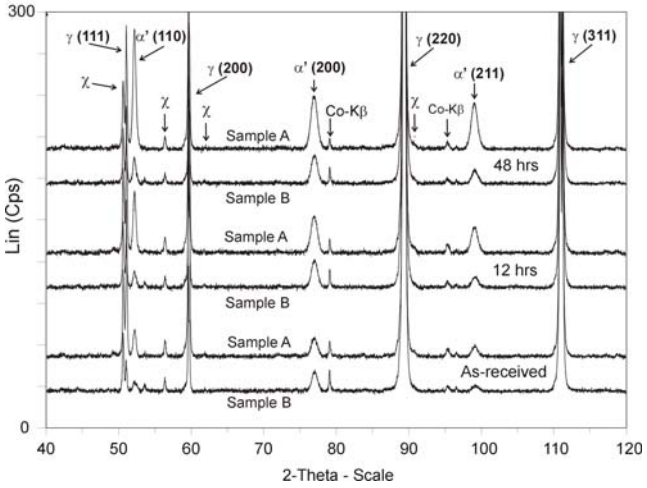

Fig. 2 X-ray diffraction profiles of samples A and B after 12 and 48 hour treatment.

Table 2. Volume fraction of martensite measured by X-ray diffraction

	Volume fraction martensite (f_m)	
Holding time [Hr]	Sample A	Sample B
As-received	0.036	0.034
12	0.086	0.050
48	0.152	0.067

In Fig.3 the evolution of the volume fraction of martensite has been plotted against time according to *XRD* and magnetization measurements. The martensite fractions obtained with the two different applied techniques are in reasonable agreement for sample A, but show significant differences for sample B. The difference observed in sample B may be caused by preferential martensitic transformation close to the surface or by a strong texture.

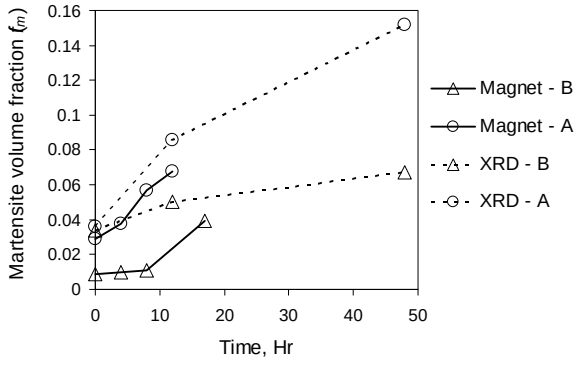

Fig. 3 Evolution of the martensite volume fraction, f_m, with time according to XRD and magnetization measurements.

Table 3. Volume fraction of martensite measured by magnetization measurements

	Volume fraction martensite (f_m)	
Holding time [Hr]	Sample A	Sample B
As-received	0.029	0.010
4	0.038	0.011
8	0.057	0.013
12	0.068	-
16	-	0.047

XRD and magnetization measurements can be used to monitor the evolution of the volume fraction of martensite but give no information about the microstructure. *3DND* measurements allow us to study the formation of martensite in a more microstructural way. *3DND* is based on the interaction of the neutron spin and the local magnetic induction in the sample. The change in polarization of a

polarized neutron beam upon transmission through the sample is characterized by the depolarization matrix *D* according to the equation *P=DP'*, with *P* and *P'* the polarized vectors before and after transmission, respectively [11, 24]. The mean magnetic induction, $\langle B \rangle$, will result in a rotation of the polarization vector around the mean magnetic induction vector. This rotation is a measure for the magnetic volume fraction and is given by $\phi = \eta L \sqrt{c} \langle B \rangle$, where $\eta = (1 - f_m)\eta^P + f_m \eta^M$ is a shape factor that accounts for the effect of strays fields; η^P the microscopic shape factor (it has a value of 0.5 for spherically shaped particles) and $\eta^M = (2/\pi)\arctan(L_Z / L_Y) = 0.5$ the macroscopic shape factor; L=0.5 mm is the thickness of the sample along the direction of the neutron beam, c=2.15×10$^{29}\lambda^2$ T^{-2}m^{-4} and λ=2.03×10^{-10} m is the neutron wavelength. The average magnetic induction in the sample can be written as $\langle B \rangle = f_m \langle m \rangle \mu_0 M_S^m$, where f_m is the volume fraction of martensite, <*m*> the average reduced magnetization in the direction of the applied magnetic field (perpendicular to the neutron beam), μ_0 = 4π×10^{-7} Hm^{-1}, and M_S^m is the saturation magnetization of martensite ($\mu_0 M_S^m \approx$ 1.8 T). The rotation angle is deduced from the matrix elements of the depolarization matrix *D*. If the value of <*m*> is known, the volume fraction can be determined. The local variations in the magnetic induction, $\langle \Delta B^2 \rangle$, will result in a shortening of the polarization vector (depolarization) by an amount proportional to the correlation function ξ of $\langle \Delta B^2 \rangle$ along the neutron path. The correlation function is a measure of the mean martensite magnetic domain size, δ, and can be written as $\xi = -\ln(\det D)/(2cL)$, where *detD* is the determinant of the depolarization matrix. In the absence of an applied magnetic field, the correlation function can be written as $\xi = (1/2) f_m (\mu_0 M_S^m)^2 \delta$ when a spherical magnetic domain of size δ and a randomly oriented domain magnetization are assumed [25]. However, in the presence of an external magnetic field, this expression should be slightly modified because some magnetization has been induced. For low values of $f_m \langle m \rangle^2$ the correlation function is now $\xi = [3/(4\gamma_Z + 5)] f_m (\mu_0 M_S^m)^2 \delta$ [25], where $\gamma_Z = 1 - [2 \ln D_{ZZ} / \ln(\det D)]$ gives which fraction of the total variation in the magnetic induction in the sample oriented along the *z* axis.

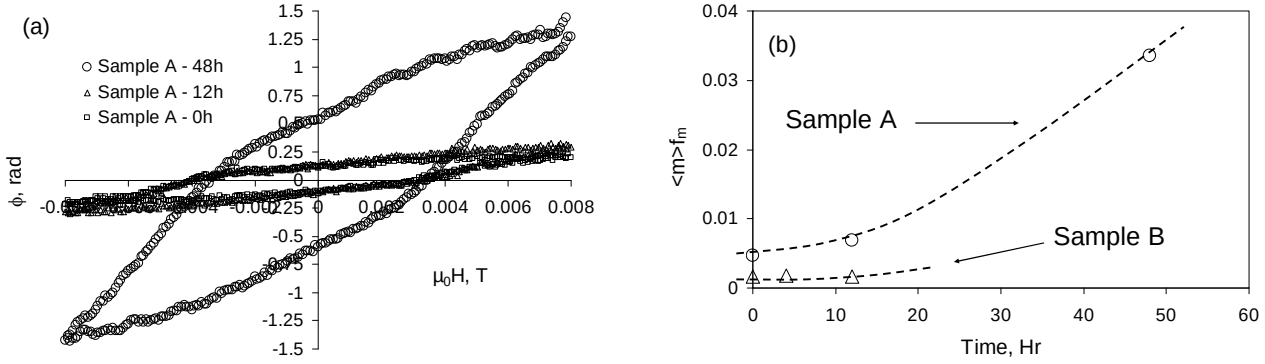

Fig. 4 Evolution of (a) the rotation and (b) the product <*m*>f_m with magnetic field for sample A.

In Fig. 4a the evolution of ϕ with magnetic field has been shown for sample A. During these measurements, the saturation rotation has not been reached in magnetic fields up to 8 mT. In Fig. 4b the evolution of <*m*>f_m has been represented with time for samples A and B assuming spherical particles (η^P = 0.5 [11]), and for an applied magnetic field of $\mu_0 H$= 8 mT. This figure provides a means to compare the evolution of the volume fraction of martensite. Trends observed are in good agreement with results shown in Fig. 3. A comparison with the magnetisation data gives a reduced magnetisation of <*m*> = 0.142±0.05 for sample A and <*m*> = 0.012±0.002 for sample B.

3DND allows us also calculating the average magnetic domain size of the ferromagnetic microstructures; in this case, martensite. The magnetic domain size has been estimated using the values of the volume fraction obtained previously with *XRD* and magnetization measurements. The derived domain size is shown in Fig.5a for sample A with and without an external magnetic field. If the saturation conditions had been attained, the system would show $<m>\sim 1$ and the domain size would be of the order of martensite plates (at least for low volume fraction of martensite where interaction between plates is minimized). In Fig. 5b the reduced magnetization has been represented for sample A. It has been calculated using the values of volume fraction of martensite from *XRD* and magnetization measurements and assuming $\eta^P = 0.5$. Since $<m>$ is lower than one, multi-domains might be present inside each martensitic plate and thus, the domain size measured (Fig. 5a) will be lower than the martensitic plate size. Taking the magnetic domain size, δ, as the diameter of a spherical martensitic magnetic domain, the volume of domains in the microstructure would be 0.18 and 0.05 μm^3 with and without an external magnetic field, respectively. On the other hand, if the AGS is taken into account (5 μm) we can expect that martensite plates to have dimensions of 3 μm × 0.3 μm × 0.3 μm and, therefore, the mean volume of a plate would be 0.27 μm^3. This estimate suggest that the magnetic domains are indeed smaller that the martensite plates. Fig. 5a also shows that the application of a magnetic field has resulted in the movement of some magnetic domains walls inside martensite plates, increasing the size of domains. Further experiments to characterize the martensitic microstructure in samples A and B are ongoing and results will be reported somewhere else.

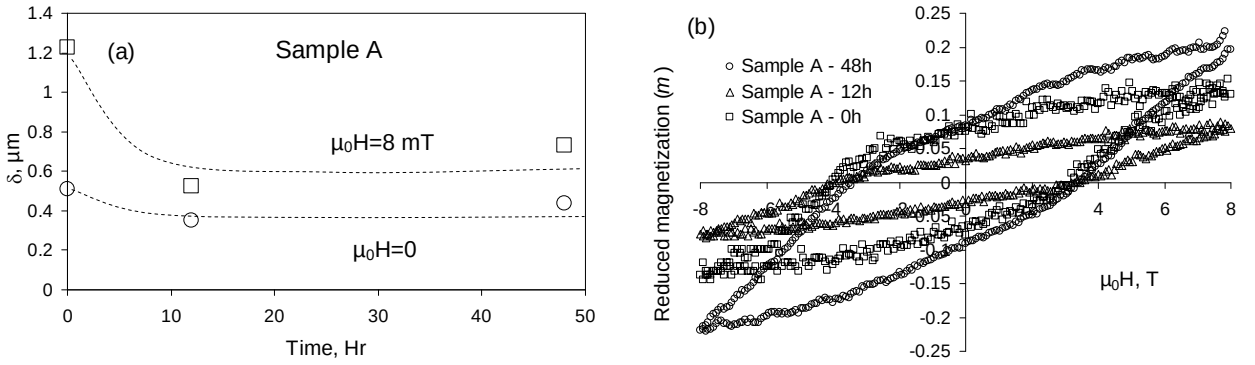

Fig. 5. (a) Evolution of the magnetic domain size of martensite with time for sample A and (b) variation of the reduced magnetization inside sample A with magnetic field

As it has be shown so far, *XRD*, magnetization, and neutron depolarization measurements can provide a complete characterization of the martensitic transformation, and show that the transformation behaviour is indeed different for the studied positions in the as-received material. However, the results do not directly explain the origin of this difference. Two main factors influence the martensitic transformation kinetics for a given composition: (1) the grain size and (2) the interstitial impurities [5, 14]. Since the austenite grain size is the same in all samples, the state of interstitials (precipitated or in solid solution) might alter the stability of austenite and be responsible for the observed differences in the martensitic transformation behaviour. Therefore, internal friction measurements have been used before to study the presence of interstitials in solid solution in steels [16-19]. Fig. 6 shows the characteristic *IF* spectrum for sample A and B obtained under the described experimental conditions. In the range of temperatures studied two main peaks have been detected. They are labelled P_{MT} and P_{INT}. Peak P_{MT} develops in both samples in the temperature range between 170 and 290 K; and peak P_{INT} has been observed between 430 and 490K. Although peak P_{MT} has been observed in the same range of temperatures in both spectra, the shape of the curve is different for both samples, implying some differences in the relaxation process associated with these peaks. The peak height, Q_m^{-1}, and the peak temperature, T_m, are different for both samples and, in sample B, only peak P_{INT} has been detected. Fig. 6b shows the internal friction spectrum

after a background correction. Table 4 lists the peak height and peak temperature of the peaks detected after background has been removed. Peak P_{MT} was observed to develop in the same temperature range where isothermal martensite forms in this steel [14]. This peak has been recorded by Golovin et al. [19] and was linked to the mechanical energy loss due to the anisothermal formation of martensite. Prioul [26] and Liu [27] detected this peak in Fe-Ni-C alloys when martensite had been transformed. Due to the nature of the martensite formation (sudden diffusionless shear transformation) large stresses are induced in the material. The internal friction is attributed to the movement of austenite/martensite and martensite/martensite interphases. From the height of the P_{MT} peaks, it can be deduced that finer martensite and/or bigger volume fraction of martensite is present in sample A compared to sample B. Moreover, the shape of peak P_{MT}^{A} suggests that a secondary peak is hidden under the main peak at lower temperatures. The corresponding peak temperature would in this case be around 190-200 K. The presence of two different P_{MT} peaks in sample B and the shift in peak temperature suggests that different types of martensite might be forming in these samples (tetragonal and/or hexagonal martensite [28]).

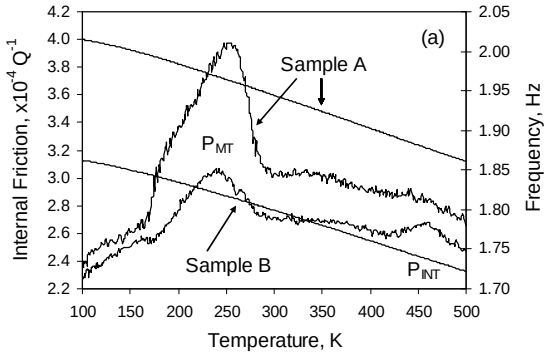

Fig. 6. Internal friction spectrum of the maraging steel studied.

Table 4. Peak height and peak temperature of the internal friction spectrum in samples A and B after background has bee removed.

Peak	T_m [K]	Q_m^{-1}, $\times 10^{-4}$
P_{MT}^{A}	255	1.013
P_{MT}^{B}	240	0.376
P_{INT}	462	0.131

Peak P_{INT} in sample B develops in the same range of temperatures as the cold work peak (Snoek-Koster) associated with the interaction of carbon and nitrogen with dislocations in α-iron [29]. This peak has been reported also by Bagramov et al. [18] in carbon steel martensite without prior cold work. They found that it was related to the presence of martensite because it disappeared when the sample was tempered. Its height increased as a result of cold work, and therefore had to be related with the presence of dislocations. In the present steel, the fresh dislocations formed during martensitic transformation on heating can interact with free interstitials present in the matrix. Assuming that dislocation-interstitial interaction are the dominant mechanism causing the P_{INT} peak and considering that fresh dislocation are present in both samples, the spectrum suggests that free interstitials are present in sample B but not present in sample A. On the other hand, the combined existence of peak P_{INT} along with smaller peak P_{MT} in sample B in comparison to sample A, suggests that the presence of interstitials in solid solution in sample B, stabilizes the austenite, retarding its transformation to martensite. On the contrary, in sample A, interstitials are not present and their effect on the martensitic transformation is negligible.

Summary

The martensitic transformation behaviour has been studied in a 12Cr-9Ni-4Mo maraging steel using *XRD*, magnetization, and *3DND* measurements. *XRD* and magnetization measurements allow the determination of the volume fraction of martensite. *3DND* can monitor both the volume fraction and the magnetic domain size of martensite, which can be related to the martensite plate size. Bearing in mind that the austenite grain size is the same in both samples, internal friction measurements suggest that the presence of interstitials in solid solution affect the transformation behaviour. Local

differences in solute interstitials levels could explain the observed local differences in transformation behaviour. Internal friction is shown as a powerful technique to characterize both, the martensitic transformation as well as the amount of interstitials in solution.

Acknowledgements

The authors are grateful to the *Stichting voor Fundamenteel Onderzoek der Materie* (*FOM*) and the Netherlands Institute for Metals Research (*NIMR*) (project number 02EMM30-3) in the Netherlands for providing financial support.

References

[1] A. Borgenstam and H. Hillert: Acta Mater. Vol. 45 (1997) p. 651.
[2] E. Nagy, V. Mertinger, F. Tranta and J. Solyom: Mater. Sci. Eng. A Vol. A378 (2004) p. 308.
[3] K. Mumtaz, S. Takahashi, J. Echigoya, Y. Kamada, L.F. Zhang, H. Kikuchi, K. Ara, M. Sato: J. Mater. Sci. Vol. 39 (2004) p. 85.
[4] R.W.K. Honeycombe and H.K.D.H. Bhadeshia: *Steels, Microstructure and Properties* (Edward Arnold, 2nd Edition, Great Britain, 1995) p. 83.
[5] S. Kajiwara: Acta Metall. Vol. 32 (1984) 407.
[6] C.L. Magee: *The nucleation of martensite, Phase Transformations* (ASM, 1970) p. 115.
[7] G.B. Olson and M. Cohen: Metall. Trans. Vol. 6A (1975) p. 791.
[8] A.K. De, D. C. Murdock, M.C. Mataya, J.G. Speer and D.K. Matlock: Scripta Mater. Vol. 50 (2004) p. 1445.
[9] L. Zhao, N.H. van Dijk, E. Brück, J. Sietsma and S. van der Zwaag: Mater. Sci. Eng. A Vol. A313 (2001) p. 145.
[10] S.G.E. Te Velthuis, N.H. van Dijk, M.TH. Rekveldt, J. Sietsma and S. van der Zwaag: Acta Mater. Vol. 48 (2000) p. 1105.
[11] L.J.G.W. van Wilderen, S.E. Offerman, N.H. van Dijk, M. Th. Rekveldt, J. Sietsma, S. van der Zwaag: Appl. Phys. A Vol. 74 (2002) p. S1052.
[12] N.H. van Dijk, S.E. Offerman, J.C.P. Klaasse, J. Sietsma, S. van der Zwaag: J. Magn. And Mag. Mater., Vol. 268 (2004) p. 40.
[13] N.H. van ijk, L. Zhao, M.Th. Rekveldt, H. Fredrikze, O. Tgus, E. Brück, J. Sietsma and S. van der Zwaag: Physica B Vol. 350 (2004) p. e463
[14] M. Holmquist, J.-O Nilsson and A. Hultin Stigenberg: Scripta Metall. Mat. Vol. 33 (1995) 1367
[15] J. Strid and K.E. Easterling: Acta Metall. Vol. 33 (1985) p. 2057.
[16] J. Snoek: Physica Vol. 6 (1939) p. 591.
[17] A.S. Nowick, B.S. Berry: *Anelastic Relaxation in Crystalline solids* (Academic Press, 1972).
[18] R. Bagramov, D. Mari and W. Benoit: Phil. Mag. A Vol. 81 (2001) p. 2797.
[19] I.S. Golovin, J.-O Nilsson, G.V.Serzhantova, S.A. Golovin: J. of Alloys and Compounds Vol. 310 (2000) p. 411.
[20] J. Post, K. Datta and J. Huetink, AIP Conference proceedings Vol. 712 (2004) p. 1670.
[21] B.D. Cullity, S.R. Stock: *Elements of X-ray diffraction*, (Prentice Hall, 3rd ed, NY, 2001) p.351.
[22] Chester F. Jatczak: *Retained Austenite and its measurement by X-ray diffraction* (SAE Report SP-80/ 453/ S02.50).
[23] R.S. Tebble and D.J. Craik: *Magnetic Materials* (Wiley-Interscience, 1969).
[24] S.G.E. Te Velthuis, N.H. van Dijk, M. Th. Rekveldt, J. Sietsma and S. van der Zwaag: Acta Mater. Vol. 48 (2000) p. 1105.
[25] R.Rosman, M. Rekveldt: J. Magn. Magn. Mat. Vol. 95 (1991) p. 319.
[26] C. Prioul: J. Phys., Vol. 46 (1985) p. C10.
[27] Y. Liu: Acta Metall. Mater. Vol. 41 (1994) p. 3277.
[28] J. Post: *PhD. Thesis* (Technical University of Twente 2004).
[29] G.J. Klems, R.E. Miner, F.A. Hultgren and R. Gibala: Metall. Trans. A Vol. 7 (1976) p. 839.